

np Charge Exchange Polarimetry in GeV Region

*Measurement of analyzing powers for the reaction
p + CH₂ up to 7.5 GeV/c
and n + CH up to 4.5 GeV/c at the Nuclotron
(ALPOM2 proposal)*

N. Piskunov

ALPOM2 Collaboration

V.P. Balandin, A.E. Baskakov, S.N. Basilev, K.S. Belova, Yu.P. Bushuev, O.P. Gavrishchuk,
V.V. Glagolev, D.A. Kirillov, N.V. Kostayeva, A.D. Kovalenko, N.A. Kuzmin, A.N. Livanov,
I.A. Philippov, N.M. Piskunov, A.A. Povtoreiko, P.A. Rukoyatkin, R.A. Shindin, A.V. Shipunov,
A.V. Shutov, I.M. Sitnik, V.M. Slepnev, I.V. Slepnev, S.Ya. Sychkov, A.V. Terletskiy,
A.I. Yukaev

Joint Institute for Nuclear Research, 141980 Dubna, Moscow region, Russia

C.F. Perdrisat

the College of William and Mary, Williamsburg, VA 23187, USA

V. Punjabi

Norfolk State University, Norfolk, VA 23504, USA

M.K. Jones

Thomas Jefferson National Accelerator Facility, Newport News, VA 23606, USA

E. Brash

Christopher Newport University and TJNAF

G. Martinska, J. Urban

University of P.J. Šafarik, Jesenna. 5, SK-04154 Košice, Slovak Republic

J. Mušinsky

Institute of Experimental Physics, Watsonova 47, SK-04001 Kosice, Slovak Republic

E. Tomasi-Gustafsson

IRFU, SPhn, CEA Saclay and IN2P3/IPN Orsay, France

D. Marchand, Y. Wang

IPN Orsay, 91406 ORSAY cedex, France

J. R.M. Annand, K. Hamilton

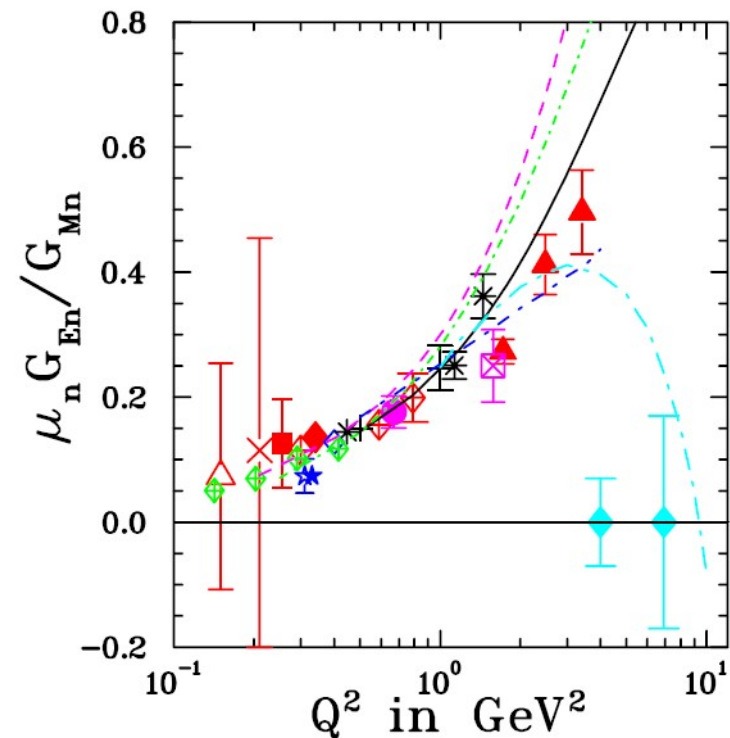
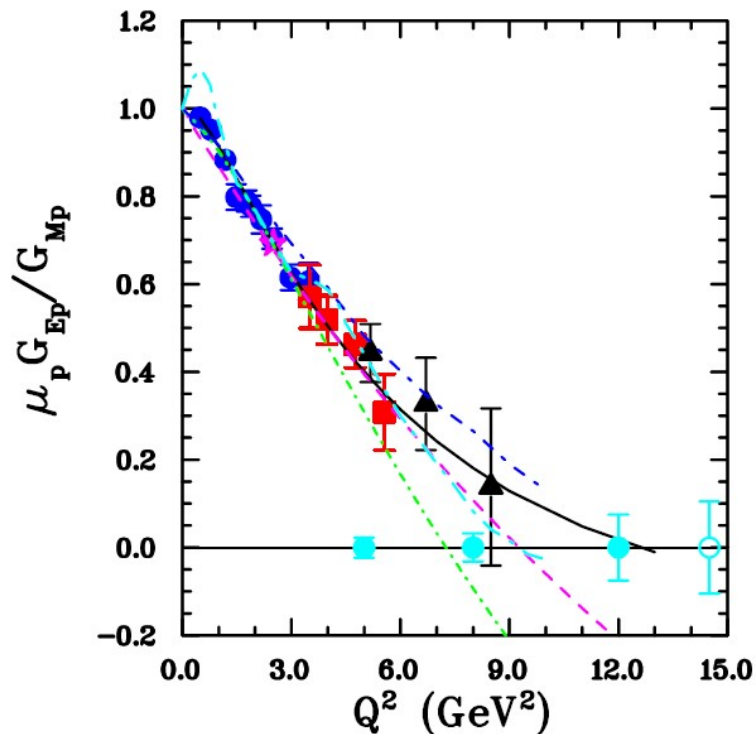
University of Glasgow, Glasgow G12 8QQ, Scotland, UK

Current Status and Projected Errors for G_{Ep}/G_{Mp} and G_{En}/G_{Mn}

Anticipated statistical uncertainties for approved experiments to measure G_{Ep}/G_{Mp} and G_{En}/G_{Mn} which will use the recoil polarization method, and CEBAF 12 GeV beam energy at JLab in near future.

The statistical uncertainty of the ratio depends directly on optimization of the coefficient of merit is ηA_y^2 . For both experiments knowledge of p and n analyzing power proposed here at Nuclotron (JINR) is of great importance.

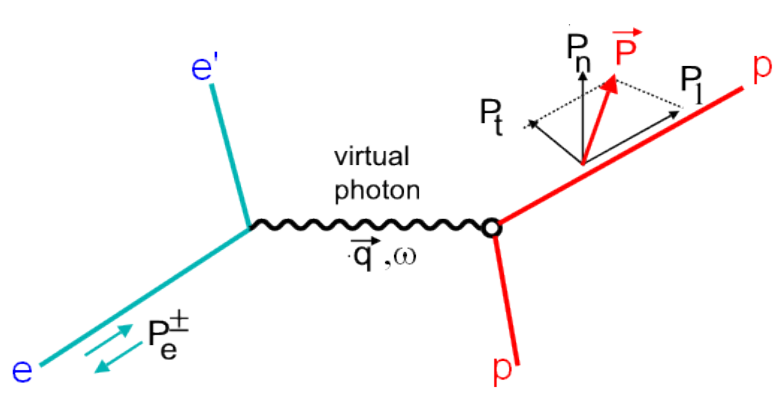
The importance of future experiments which will establish whether either ratio does, or does not cross zero near $Q^2=10 \text{ GeV}^2$.



Double Polarization Method in Elastic $\vec{e}N$ Scattering

Polarization transfer in $\vec{e}N \rightarrow e\vec{N}$ or spin-target asymmetry $\vec{e}\vec{N} \rightarrow eN$, ($N=p$ or n), two different techniques, which give same information.

For recoil polarization, the two polarization components are in the reaction plane, no normal component:



$$hP_e P_t = -hP_e 2\sqrt{\tau(1+\tau)} G_{Ep} G_{Mp} \tan\left(\frac{\theta_e}{2}\right) / I_0$$

$$hP_e P_l = hP_e \frac{(E_e + E_{e'})}{M} G_{Mp}^2 \sqrt{\tau(1+\tau)} \tan^2\left(\frac{\theta_e}{2}\right) / I_0$$

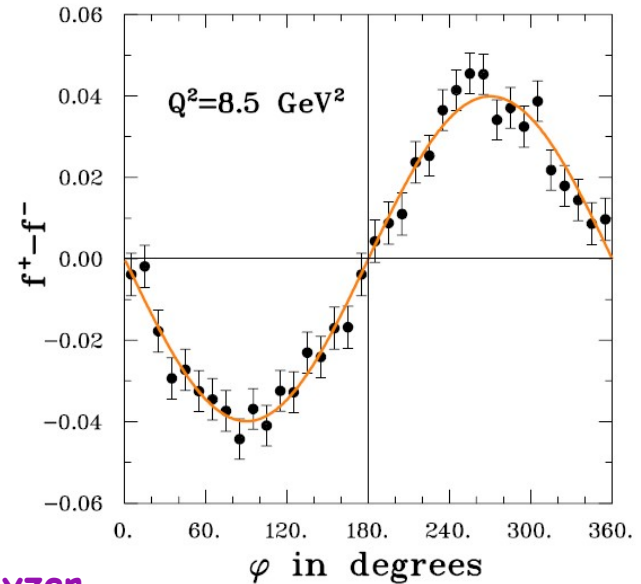
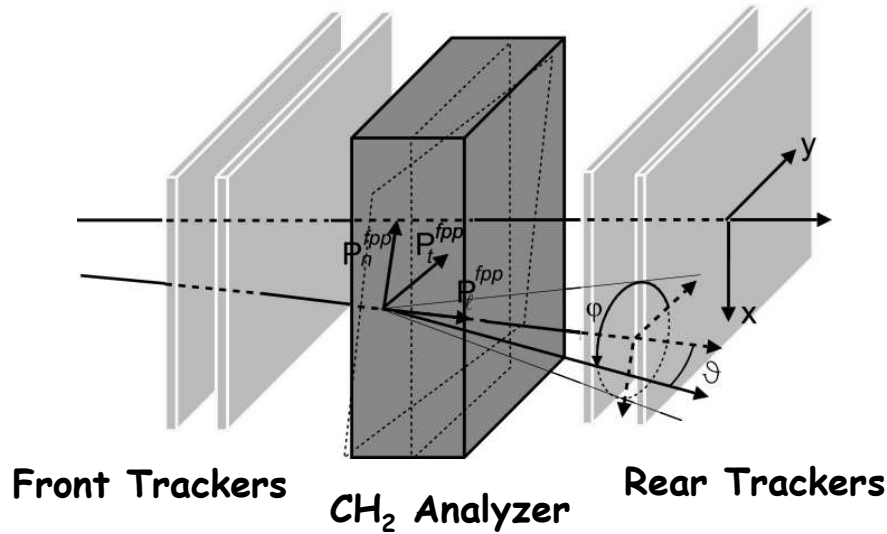
$$\frac{G_{Ep}}{G_{Mp}} = -\frac{P_t}{P_l} \frac{(E_e + E_{e'})}{2M} \tan\left(\frac{\theta_e}{2}\right) \quad \text{and} \quad I_0 = G_E^2 + \frac{\tau}{\varepsilon} G_M^2$$

Superior method: “much smaller systematics”

Form Factor ratio is independent of the electron polarization P_e and of the polarimeter analyzing power A_y (h is beam helicity ± 1).

Statistical uncertainty depends directly on both P_e and A_y .

Focal Plane Polarimeter



Azimuthal distribution of protons after scattering in the analyzer

$$f^\pm(\theta, \varphi) = \frac{\varepsilon(\theta, \varphi)}{2\pi} \left(1 \pm \bar{A}_y(\theta) P_t^{\text{fpp}} \cos \varphi \mp \bar{A}_y(\theta) P_n^{\text{fpp}} \sin \varphi \right)$$

P_t^{fpp} and P_n^{fpp} are the polarization components at the FPP

Physical Asymmetries are obtained from difference distributions

Sum distribution gives instrumental asymmetries

$$D_i = \frac{(f_i^+ - f_i^-)}{2} = \frac{\varepsilon(\theta, \varphi)}{2\pi} \left[\bar{A}_y P_t^{\text{fpp}} \cos \varphi - \bar{A}_y P_n^{\text{fpp}} \sin \varphi \right]$$

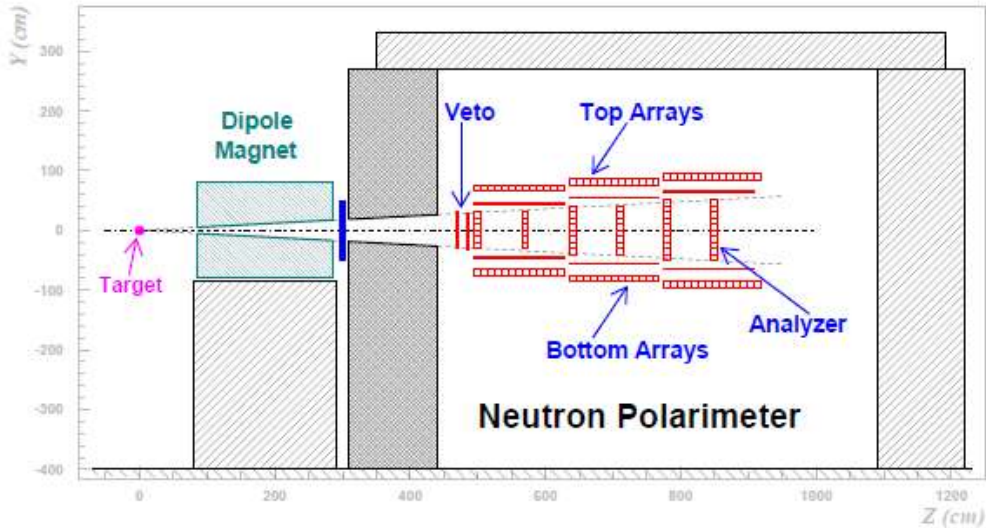
$$E_i = \frac{(f_i^+ + f_i^-)}{2} = \frac{\varepsilon(\theta, \varphi)}{2\pi}$$

The properties of the polarimeter are analyzing power A_y , and probability of elastic (or quasi-elastic scattering), η . The coefficient of merit is ηA_y^2 .

The statistical uncertainty on the form factors is $\frac{1}{\sqrt{N\eta A_y^2}}$ where N is number of events.

The Neutron Electric Form Factor at Q^2 up to 7 (GeV/c)^2
 from the Reaction ${}^2\text{H}(\vec{e}, e'\vec{n}){}^1\text{H}$ via Recoil Polarimetry

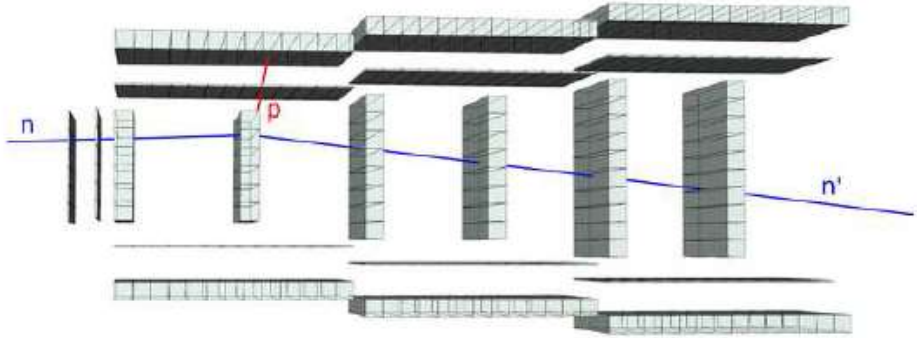
E12-11-009



CH - material

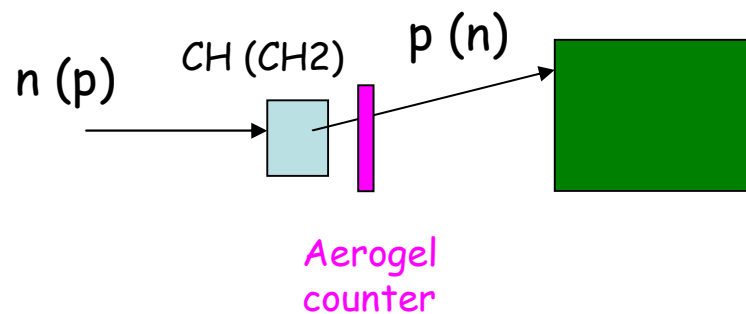
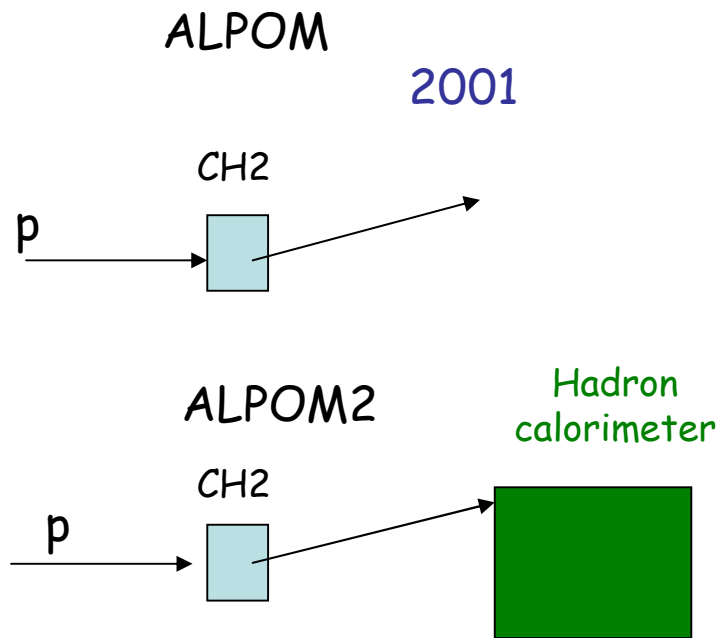
Low neutron detection efficiency

Figure 14: Neutron polarimeter to be used in the measurements.



Neutron Momentum, P_n (GeV/c)

| 2.901 | 3.602 | 4.511



$$F^2 = \int \varepsilon(\theta) A_y^2(\theta) d\theta$$

$$\Delta P_y = \sqrt{\frac{2}{N_{inc} F^2}}$$

Proton polarimetry

$p + C(CH_2) \rightarrow \text{charged particle} + X$

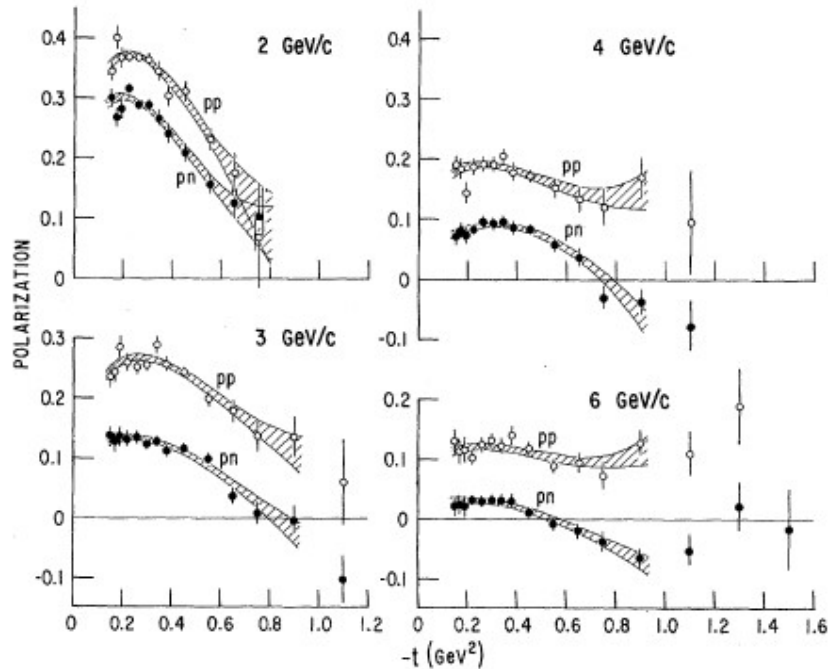
Neutron polarimetry

$n + p \rightarrow n + p$, CH - target

New suggestion: $n + p \rightarrow p + n$
Charge exchange reaction

Phys. Rev. Lett 35 (1975) 632

pp -> pp
 pd -> pn + (p)

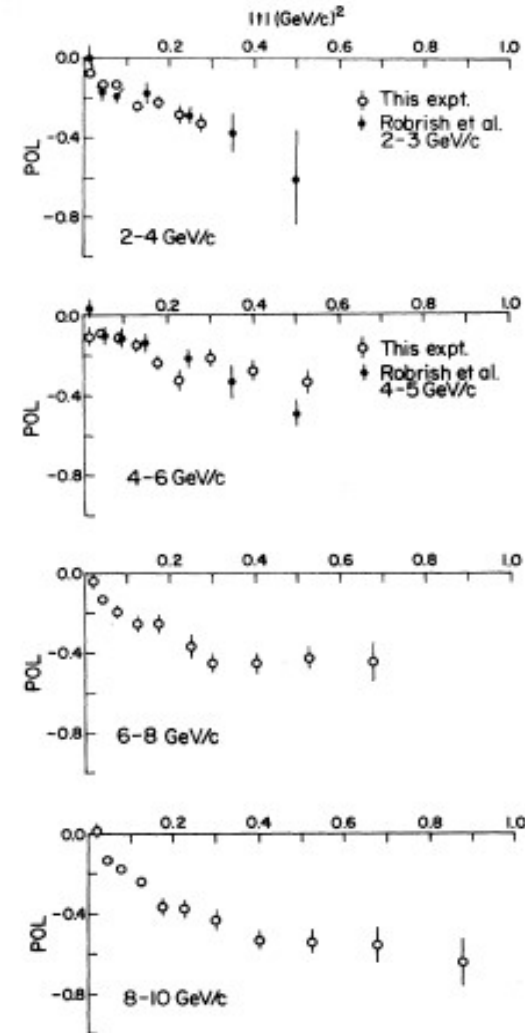


A_y decreasing with energy

The existing data for A_y in np elastic scattering indicate that the analyzing power decreases faster than the pp analyzing power, becoming very small, then negative around 6 GeV/c neutron momentum.

Phys. Rev. Lett 30 (1973) 1183

np -> pn

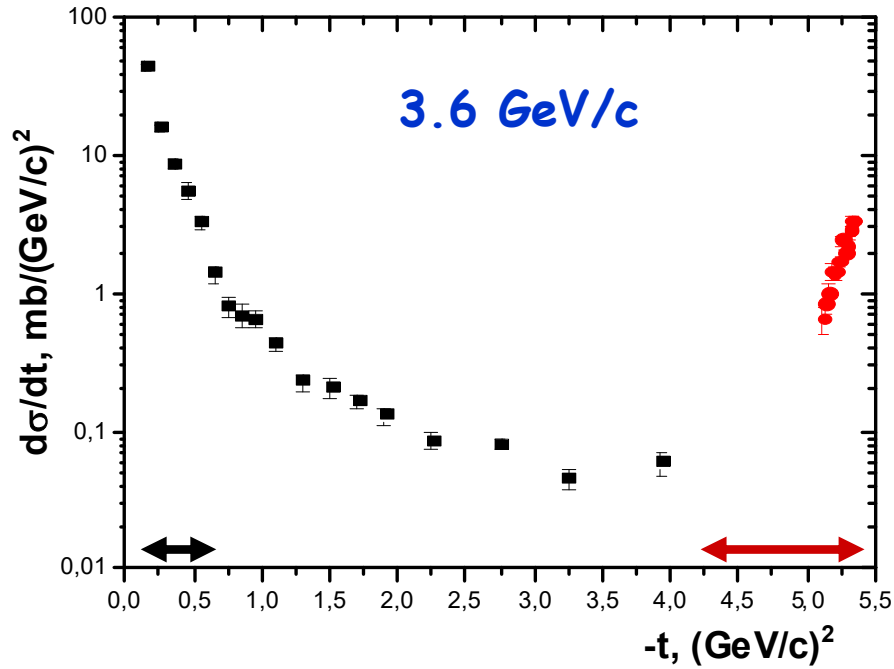


A_y increasing with energy

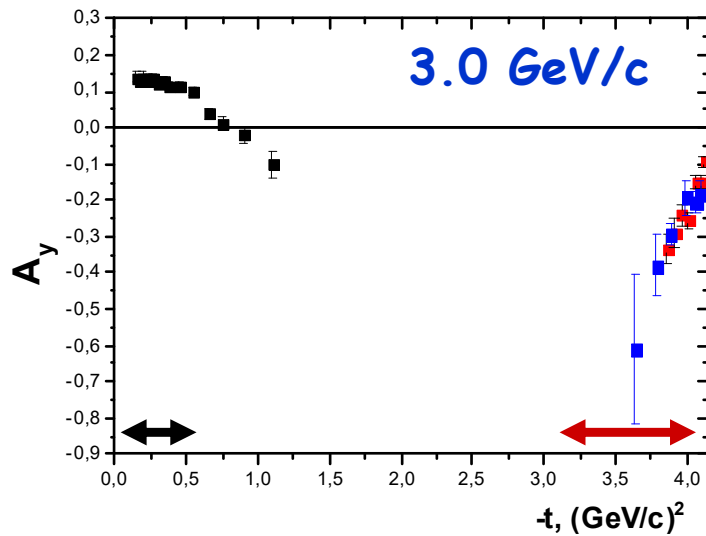
np -> np

np -> pn

Liquid H2 or D2 target



$$d\sigma/dt_{el} > d\sigma/dt_{ce}$$

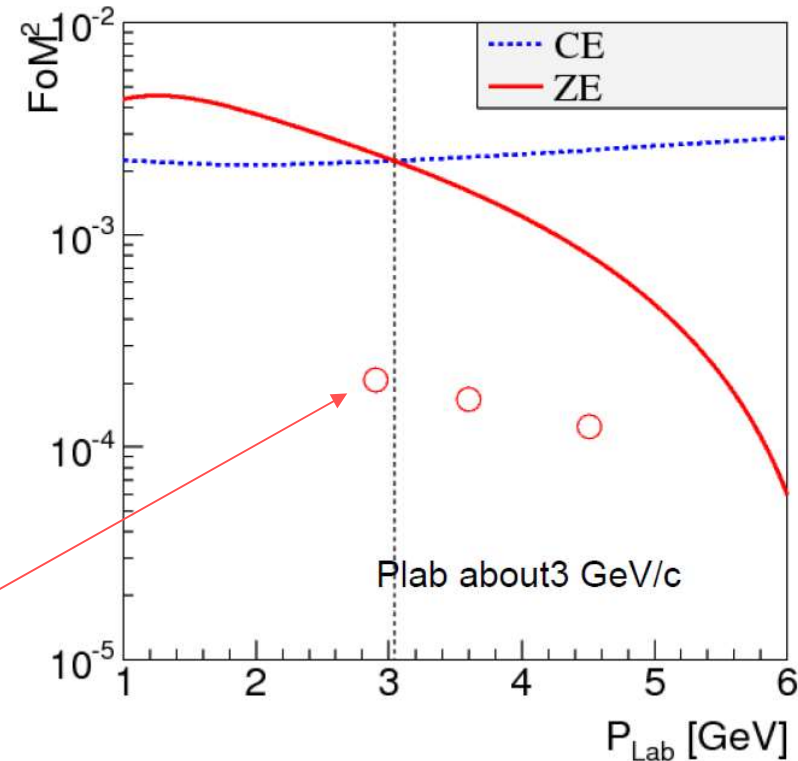


$$|A_y^{el}| < |A_y^{ce}|$$

$FOM^{el} < FOM^{ce}$
and increasing with energy

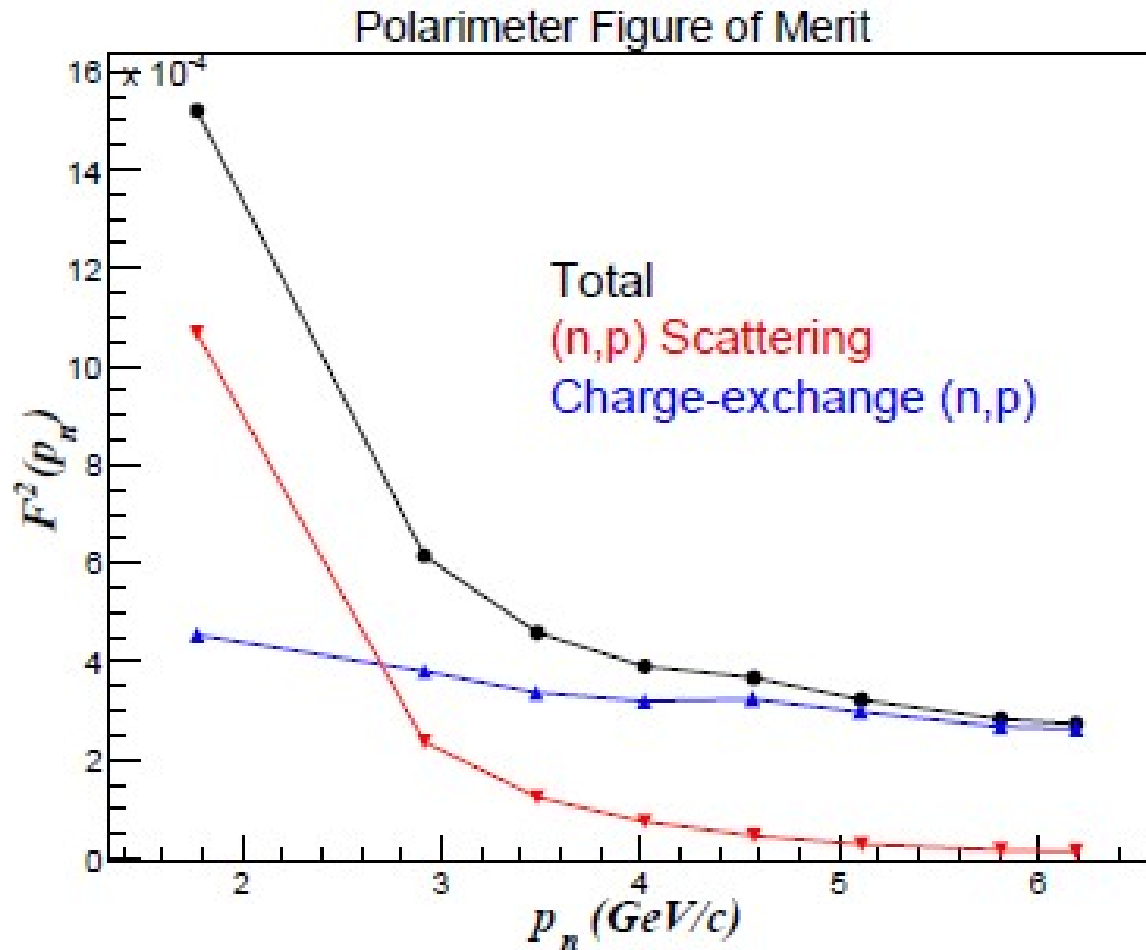
Figure of merit

From 1 to 3 GeV/c, ZE has larger Figure of merit due to its larger total cross section. After 3, as cross section becomes really small, figure of merit is dominated by analyzing power, then CE becomes bigger.



E12-11-009
CH - target

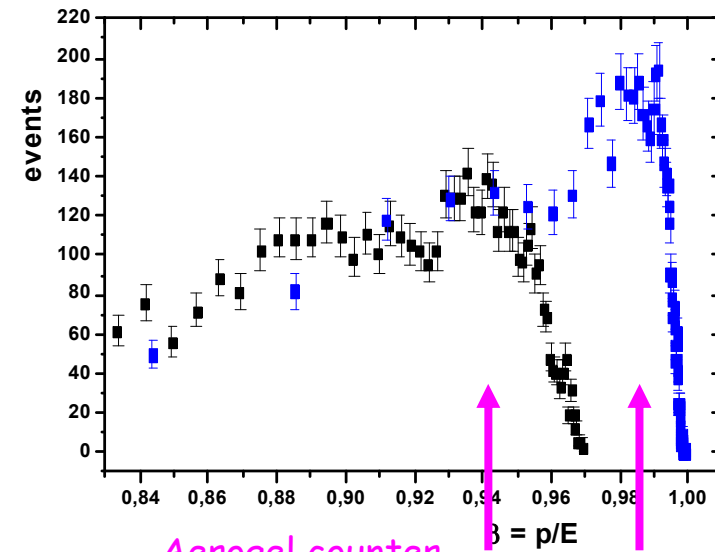
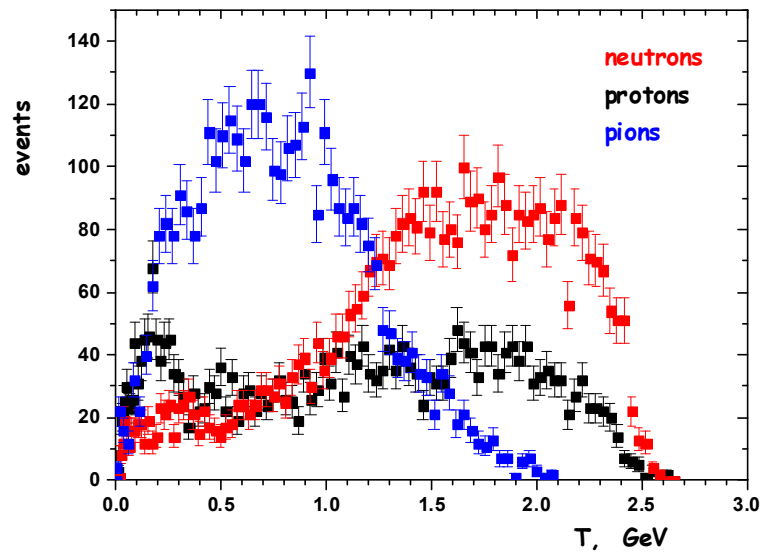
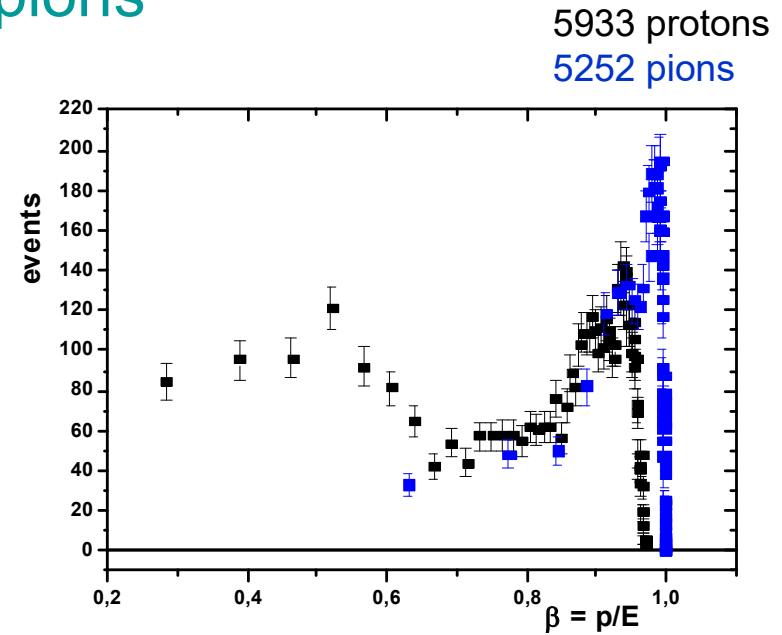
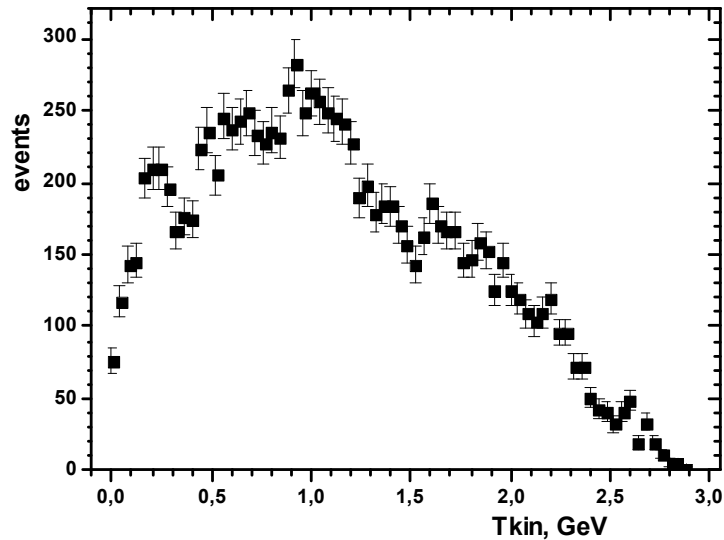
Changing CH to CH2 increases difference FOM twice



J.R.M. Annand's
calculations
for CH target

Figure 6: Neutron polarimeter figure of merit as a function of incident neutron momentum. Red: standard $n - p$ scattering, blue: charge-exchange $n - p$ scattering, black: sum of the two scattering channels.

HBC, 3.83 GeV/c protons & pions



Suppression of pions emitted from the target by aerogel counter

Aerogel counter

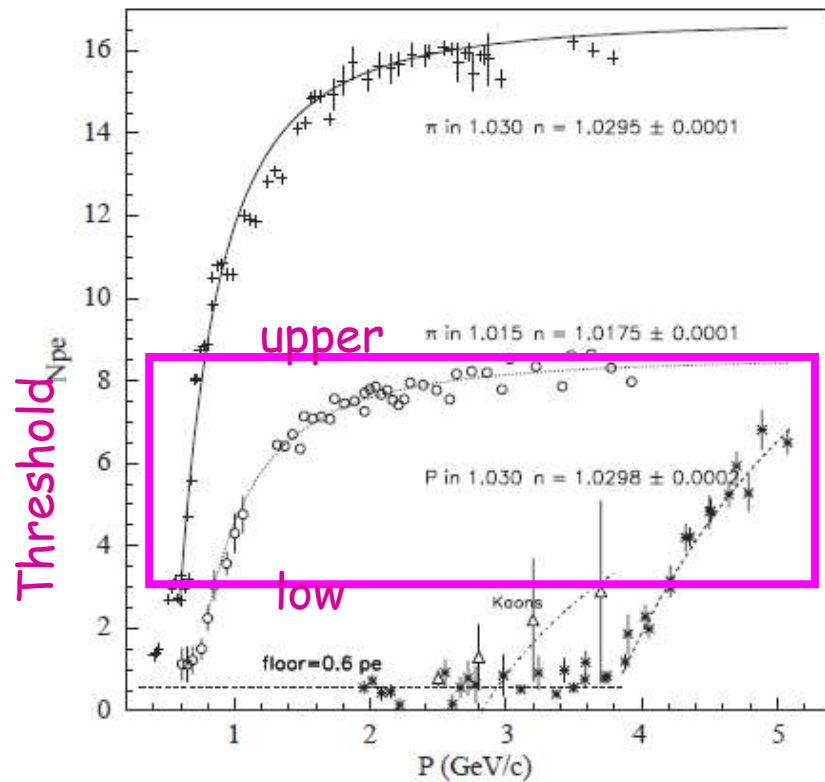


Fig. 7. The momentum dependence of N_{pe} for both types of aerogel material used and for different particles. Both the experimental data and fits to them are shown (compare to Fig. 1).

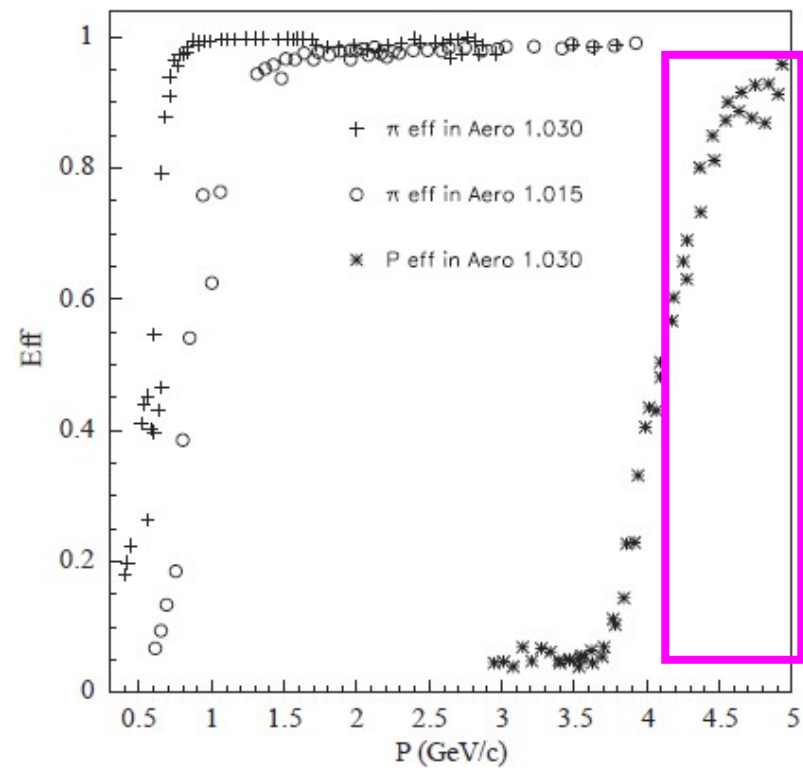
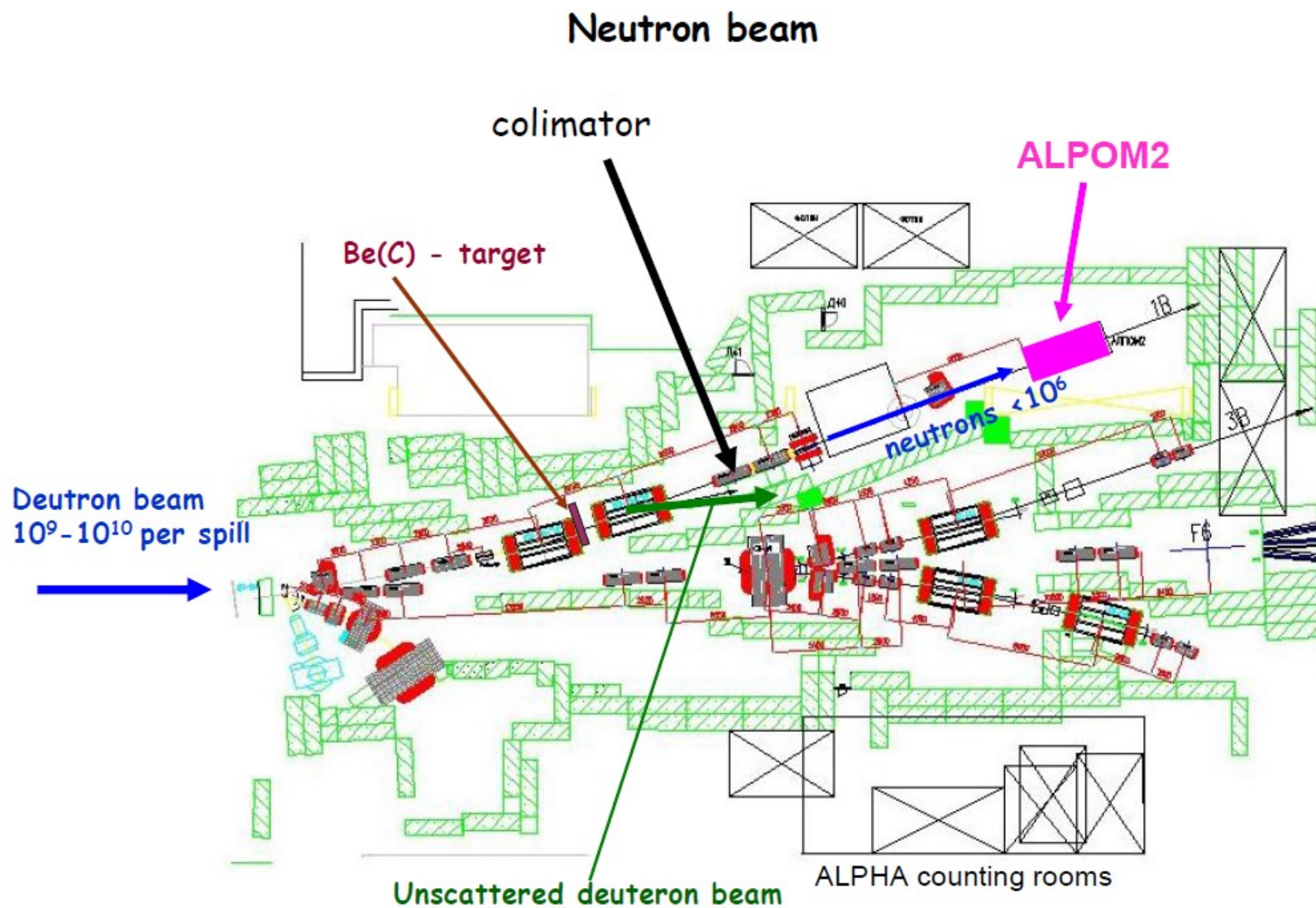


Fig. 8. Particle detection efficiency versus momentum P for the detector with aerogels $n = 1.030$ and $n = 1.015$.

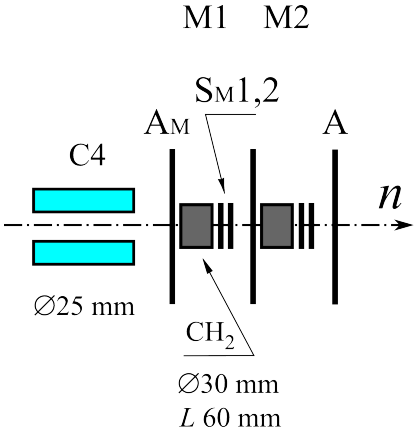
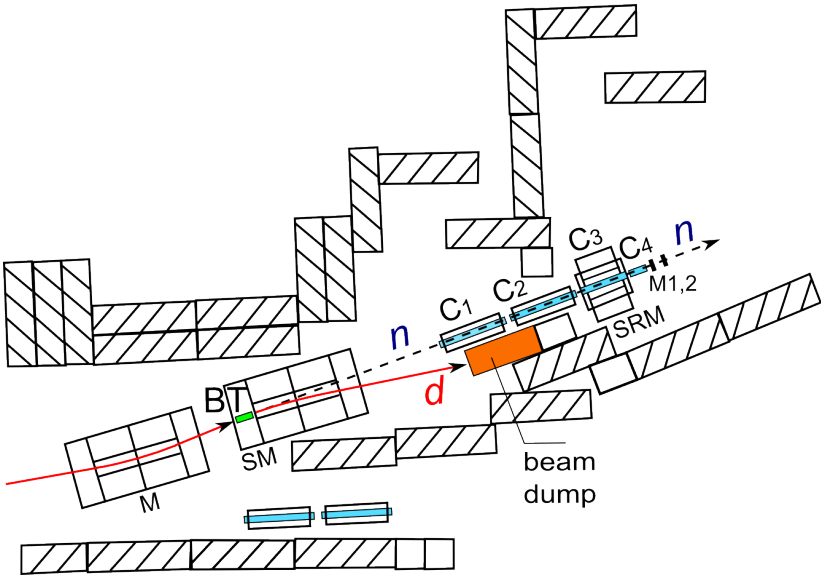
If we use this counter in the differential mode we can detect only protons in our sensitive region

Schematic of Neutron Beam Extraction and Transport



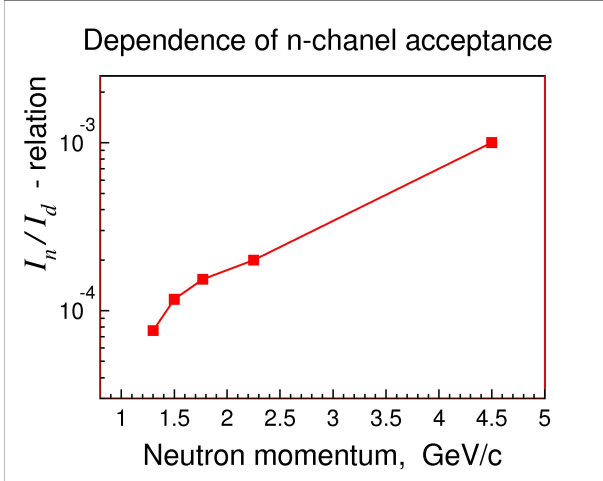
neutron monitors

Scheme of both extracted deuteron and free neutron beam lines.
 The beryllium target BT for the neutron production,
 the collimators C1 - C4, the monitors M1, M2 for estimation of
 beam intensity, the SM - magnet for vanishing of the charged deuterons.



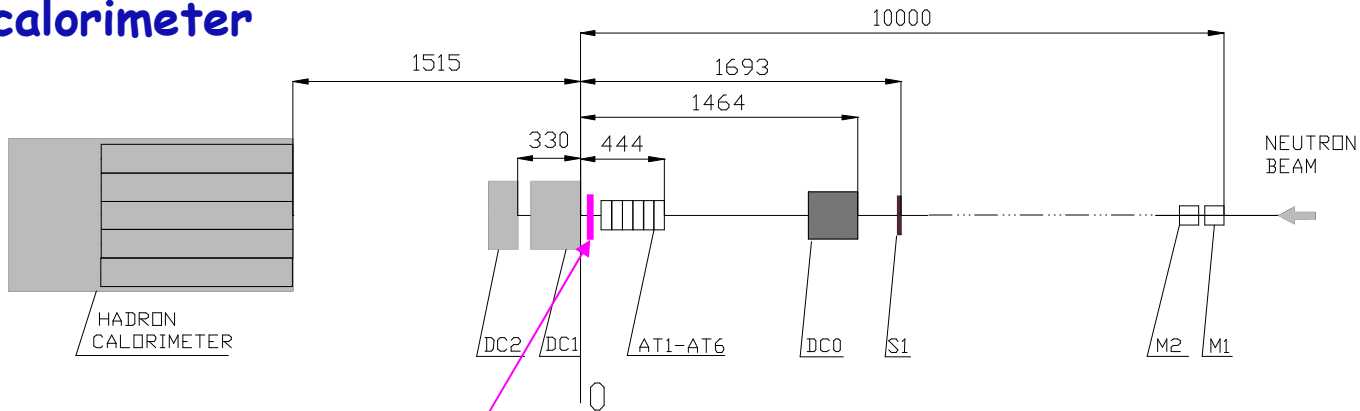
Neutrons have a laboratory momentum $P_n = P_d / 2$
 with a gaussian momentum spread of $\sigma P/P \sim 3 \div 4 \%$

The distance from the BT to the collimator exit is about 12 m
 and thus determining the solid angle equal ~ 5 msr.



Drift chambers

Hadron calorimeter



Neutron beam

Aerogel counter

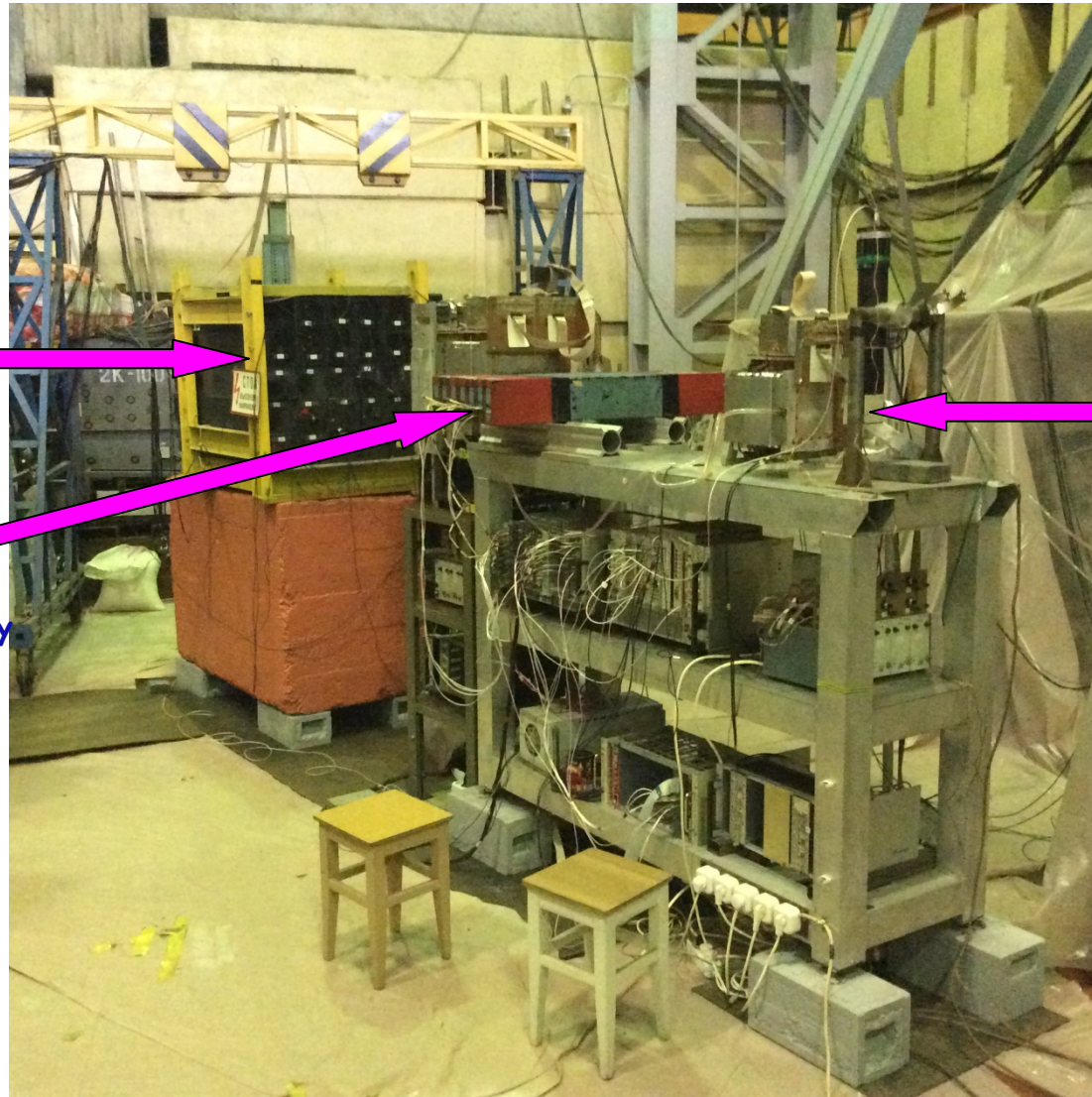
Active target
For neutron A_y
measurement

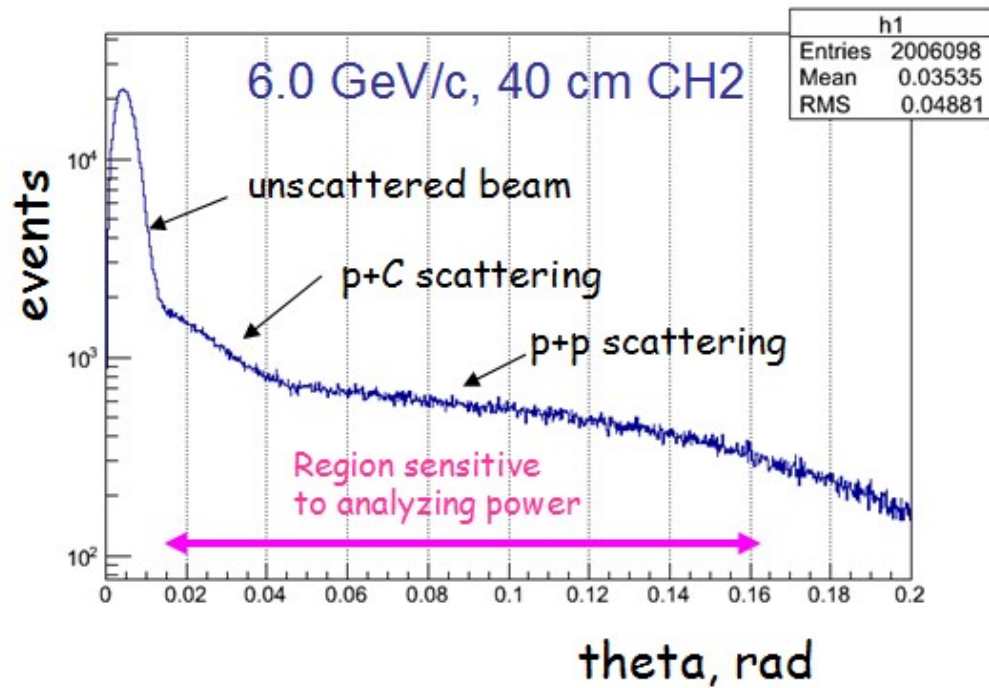
Picture of the ALPOM2 Setup

Hadron calorimeter

Neutron beam

Active target
For neutron A_y
measurement

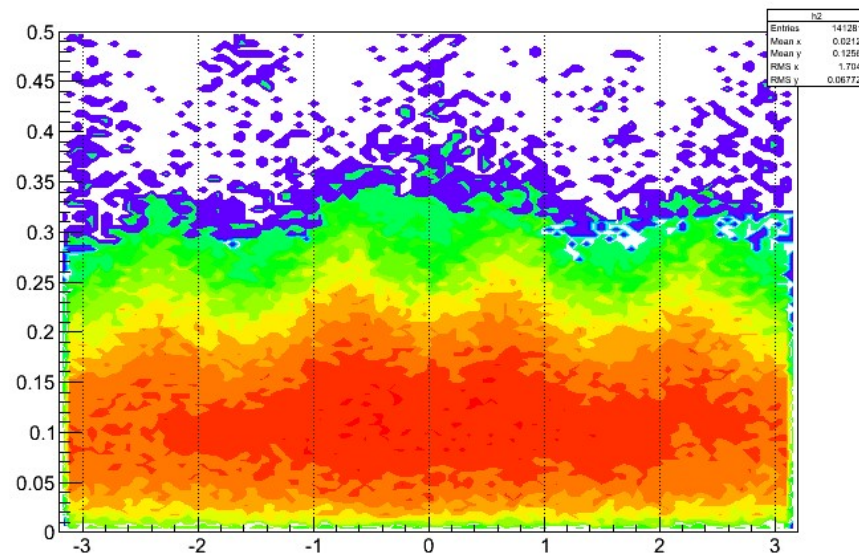
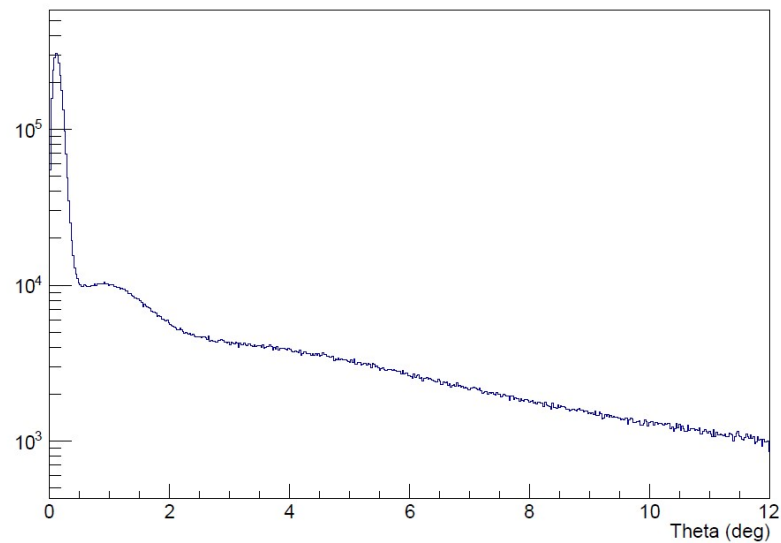




The angular distribution of charged particles after the target.

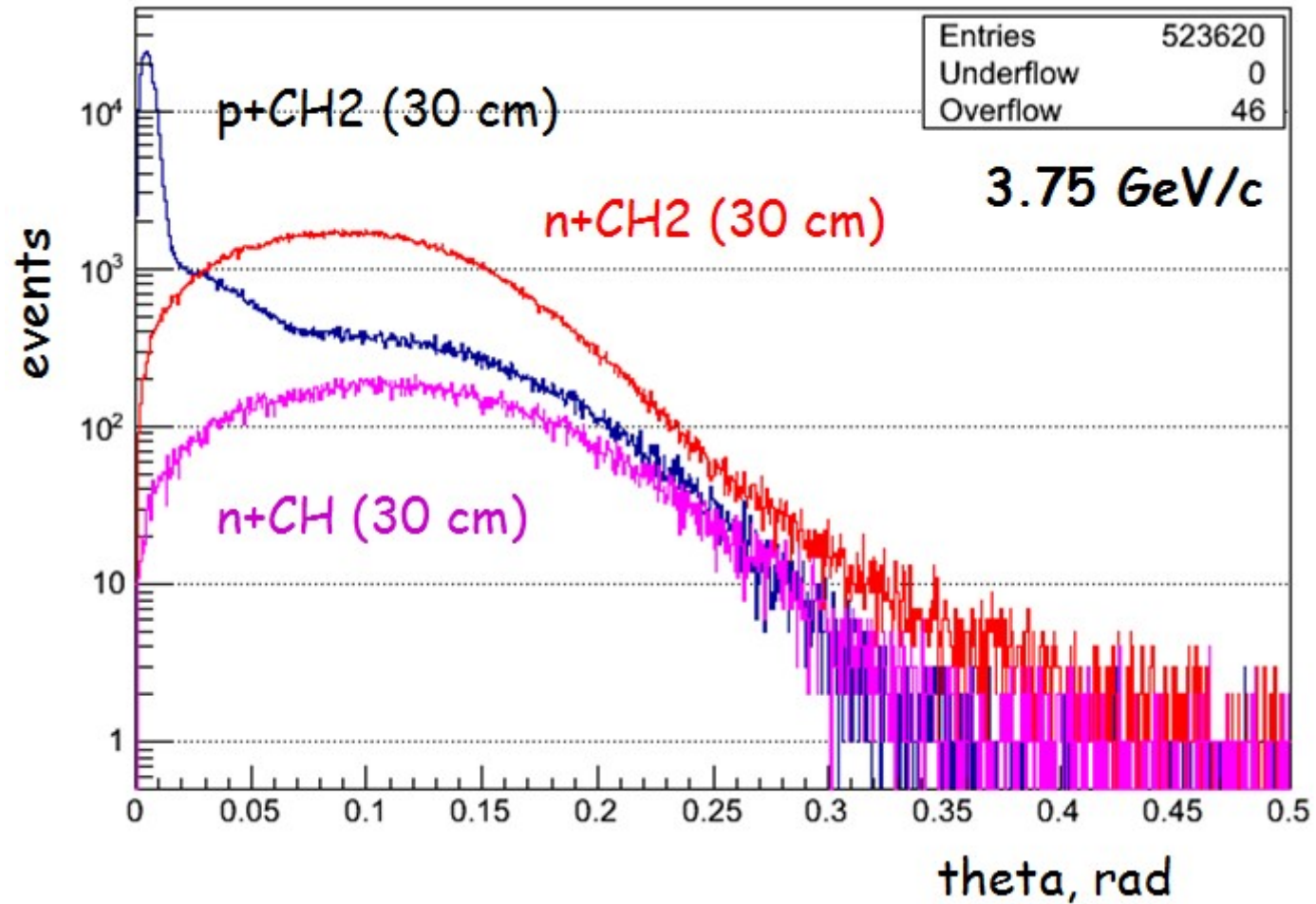
MC simulation result

protons at cal (p beam 6GeV/c)



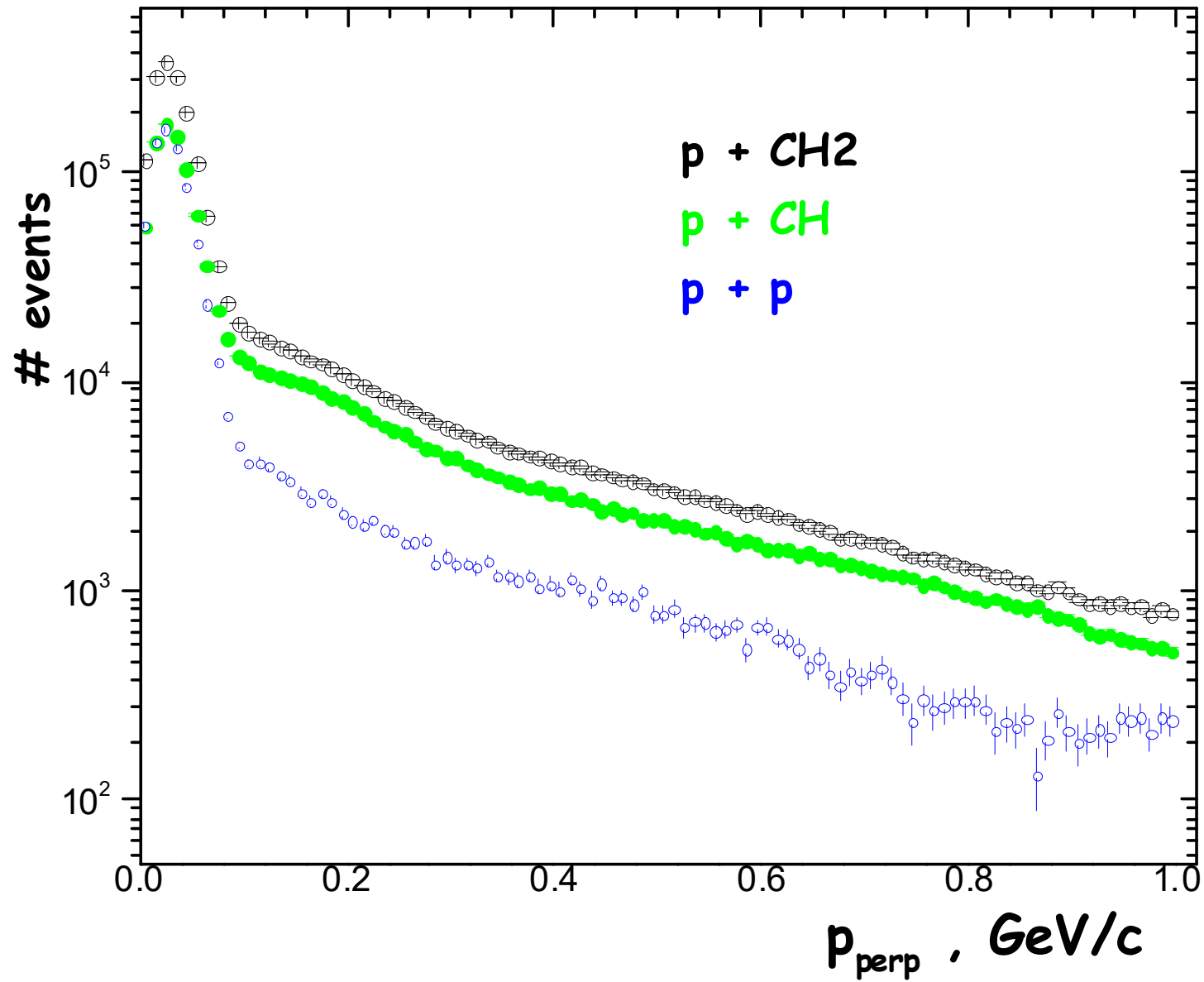
Theta-phi correlation plot.

The angular distributions of neutrons and protons with the momentum of $3.75 \text{ GeV}/c$ for CH and CH_2 targets, compared with the distribution for incident protons.



3.75 GeV/c June 2016

About 10^6 tracks



Conclusion

Charge-exchange np reaction is preferable over np elastic scattering in GeV region

A new polarized source is under tuning now

The setup has been tested

We hope that the measurements be done in 2016

Thank you for your attention

1.1 GeV

arXiv:1408.4928v1 [nucl-ex] 21 Aug 2014

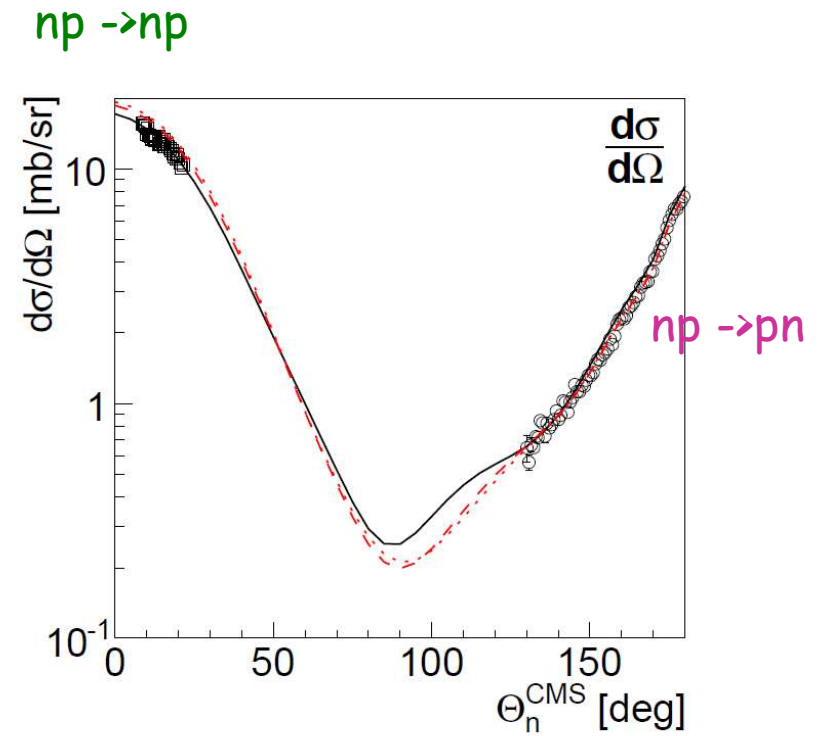
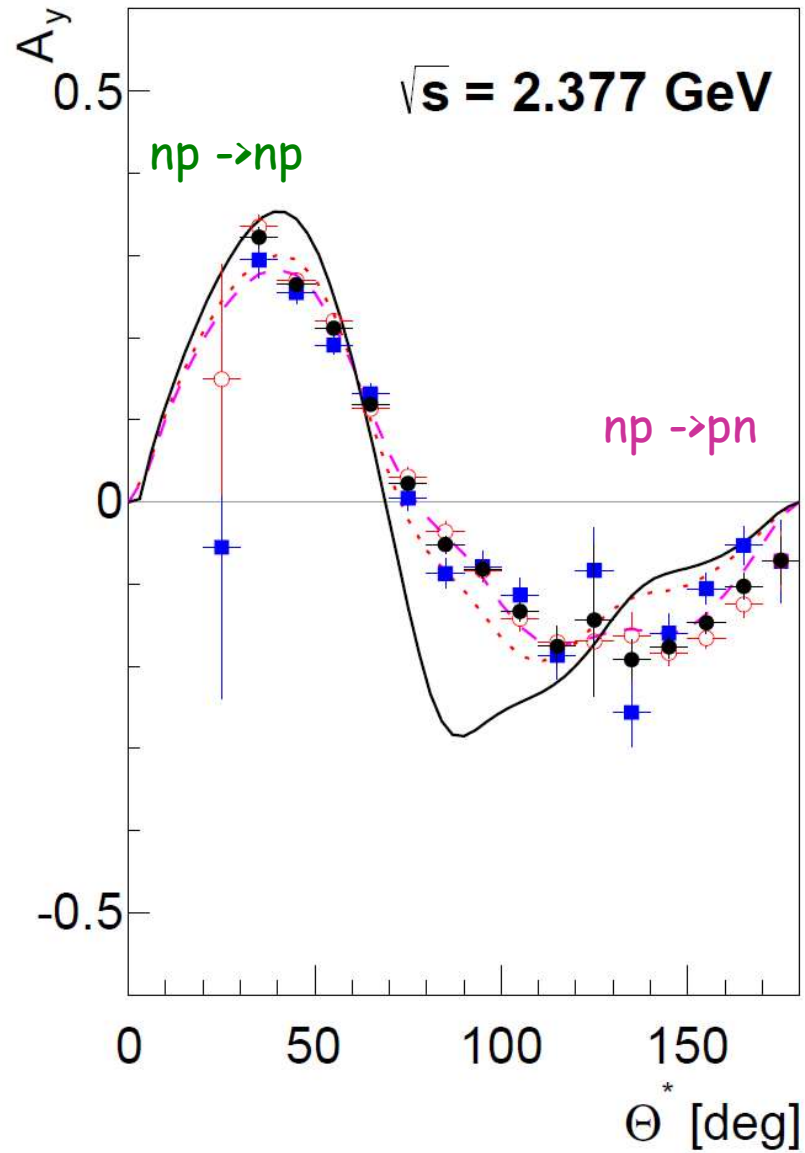
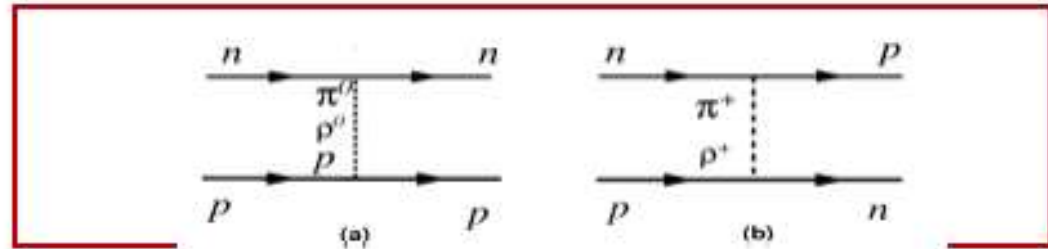


FIG. 11: (Color online) Angular distribution of the differential cross section $d\sigma/d\Omega$ at $T_n = 1.135$ GeV corresponding to the resonance energy $\sqrt{s} = 2.38$ GeV. For the meaning of the curves see caption of Fig. 4. The plotted data are from Ref. [41] ($T_n = 1.135$ GeV) and Ref. [42] ($T_n = 1.118$ GeV).

Pole model for reactions $np \rightarrow np$ (pn)

Neutron

➤ Differential cross section



$$\frac{d\sigma}{dt} = \frac{1}{64\pi s q^2} (|T_\pi(u) + T_\rho(u)|^2 + \frac{1}{4} |T_\pi(t) + T_\rho(t)|^2 + |T_P(t)|^2)$$

$$|T_{CE}(u)|^2 = \left(F_u \frac{u A_\pi}{u - m_\pi^2} F_u \right)^2 + \left| F_u \frac{u A_\rho e^{i\varphi}}{u - m_\rho^2} F_u \right|^2 + 2 \left(F_u \frac{u A_\pi}{u - m_\pi^2} F_u \right) \left(F_u \frac{u A_\rho e^{-i\varphi}}{u - m_\rho^2} F_u \right)$$

$$|T_{ZE}(t)|^2 = \frac{1}{4} \left[\left(F_t \frac{t A_\pi}{t - m_\pi^2} F_t \right)^2 + \left| F_t \frac{t A_\rho e^{i\varphi}}{t - m_\rho^2} F_t \right|^2 + 2 \left(F_t \frac{t A_\pi}{t - m_\pi^2} F_t \right) \left(F_t \frac{t A_\rho e^{-i\varphi}}{t - m_\rho^2} F_t \right) \right] + (A_P e^{-\theta|t|})^2$$

Yu.A. Troyan, M.Kh. Anikina, A.V. Belyaev, A.P. Ierusalimov, and A.Yu. Troyan.
Elastic $np \rightarrow np$ (pn) scattering at intermediate energies. *Physics of Particles and Nuclei Letters*, 11(2):101–108, 2014.

Differential cross section

